Research Article

Adsorption of Phenolic Compounds from an Aqueous By-product of Sunflower Protein Extraction/Purification by Macroporous Resins

Tuong Thi Le[1,2], Aymes A[1], Framboisier X[1], Ioannou I[1,3], Kapel R[1*]

[1]Laboratory of Reactions And Chemical Engineering, University of Lorraine, Nancy, France; [2]Laboratory of Stress Immunity Pathogens, University of Lorraine, Nancy, France; [3]URD Industrial Agro-Biotechnologies, AgroParisTech, CEBB, France

ABSTRACT

In this study, adsorption of phenolic compounds from an aqueous by-product of sunflower protein isolate production was investigated. Phenolic compounds in this by-product (ultrafiltration permeate of protein purification step) were almost exclusively CGA (mainly 5-CQA isomer). Five different macroporous resins including XAD4, XAD7, XAD16, XAD1180, and HP20 were screened for CGA capture. XAD16 had the best massic adsorption capacities (15.32 ± 0.04 mg/g), while XAD7 had a better surface adsorption capacity (0.027 ± 0.00146 mg/m²). CGA adsorption on both resins followed the pseudo-second-order kinetic model with a similar intra diffusional pattern. Adsorption isotherms of the two resins better fitted the Langmuir model with Qmax for XAD7 and XAD16 of 0.054 and 0.040 (mg/m²), respectively. The adsorption process of phenolic compounds revealed to be exothermic, physical adsorption, and spontaneous. Better adsorption results were observed at 25°C. Maximal CGA desorption ratio was observed from 70% (v/v) ethanol. The high values were reached with both the resins (88.09 ± 0.13 and 86.16 ± 0.32% for XAD7 and XAD16, respectively). The CGA purity in the desorption phase was surprisingly high (77.56 ± 0.99% and 74.59 ± 0.12% for XAD7 and XAD16, respectively).

Keywords: Sunflower meal; Macroporous resin; Adsorption study; Chlorogenic acid.

INTRODUCTION

Phenolic compounds are a wide group of natural products from plant sources. These molecules are secondary metabolites having one or several benzene ring with hydroxyl groups. They are known to have various bioactivities like antioxidant, anti-inflammatory, anti-cancer, anti-ageing, or anti-osteoporosis activities [1-3]. Among phenolic compounds, chlorogenic acid (CGA) revealed particularly attractive. Chemically, CGA is a polar phenolic compound composed of a quinic acid and caffeic acid linked by an ester bond. The position of the quinic acid on the benzene ring define three CGA isomers including 5-O-caffeoylquinic acid i.e 5-CQA, 4-O-caffeoylquinic acid i.e 4-CQA, and 3-O-caffeoylquinic acid i.e 3-CQA. Interestingly, CGA has demonstrated high anti-oxidant, anti-inflammation and anti-tumor effects [4,5]

Some raw materials like coffee beans, low-grade coffee beans, noxious weeds like Eupatorium adenophorum Spreng (Crofton weed) [6] or Boehmeria nivea L. Gaud (Ramie) leaves [7] revealed to be interesting sources of CGA. Sunflower seed is also rich in phenolic compounds (14.5% on a dry weight basis) and particularly in CGA. It is the second most cultivated oilseed in Europe with an annual production of about 16 million tons (FAO, US Department of Agriculture) in 2018 [8]. It is mainly processed for oil production. The industrial oil extraction process yields a solid by-product called "meal" composed of up to 50% of proteins [9,10], which contains seeds phenolic compounds. Beside CGA, these compounds are mainly CGA isomers, CGA dimers, and caffeic acid.

To date, sunflower meal is mainly used for the feed. For this purpose, phenolic compounds are considered as antinutritionals and need to be eliminated. Many approaches were reported to remove phenolic compounds from the meal. As for other resources, the most classical way is to use organic solvents like acetone, methanol, ethyl acetate or water/ ethanol mixtures [11,12]. Weizs GM et al. 2009 [13] showed that methanol/water mixtures 60% (v/v) was suitable for extraction of sunflower phenols from both kernels and shells. Interestingly, they showed that the obtained extract with a phenolic fraction composed of a particularly high proportion of CGA (around 85%). After solvent extraction, phenolic compounds can be further purified by chromatography [14], membrane processes [15,16] or adsorption on macroporous resins [17]. This last process proved to be particularly efficient for phenolic compounds capture from various plant extracts [6,17,18]. Besides, adsorption processes can easily be scaled up and some resins are food grade [19]. Macroporous resins are divided into polar resins, mild polar resins, and non-polar resins. The mechanism of separation is based on differential affinity between phenolic compounds, impurities, and the adsorbent [20]. Proper

resins should be chosen based on both adsorption capacities and purity after desorption step, but purity is often not considered. Furthermore, the complex transport phenomenon that are also involved are rarely thoroughly investigated.

Sunflower meal is also considered as an promising source of proteins [21,22] for food applications under isolate products. The production of sunflower protein isolates is classically achieved in two main steps (aqueous extraction and purification). The extraction step has to be done under pH 8 and at high NaCl concentration (> 0.2 M NaCl) in order to get satisfying protein extraction yield and color [23,24]. A large part of sunflower phenolic compounds are extracted alongside with proteins in these conditions. Recently, an integrated process was proposed for both protein and phenolic compounds valorization [25,26]. This process integrates a capture of phenolic compounds by adsorption from the aqueous extract prior to protein purification by acid precipitation. The resin had to have low protein binding capacity. XAD16 resin revealed to be the most appropriate resin to do so beyond other apolar and ion exchange resins [26]. However, CGA purity after adsorption step was not considered and adsorption mechanisms and transport were not investigated and remained unclear. Furthermore, in this approach, protein acid precipitation led to an isolate having a poor solubility which is rather detrimental for food applications.

More recently, we proposed an alternative approach in which sunflower proteins are purified from the aqueous extract by tangential filtration [27]. This yielded a highly soluble sunflower protein isolate with high functional properties. Interestingly, phenolic compounds in the extract were only composed of CGA (mainly 5-CQA isomer) [27]. The liquid effluent of this process (the UF permeate) was largely depleted in proteins and probably contained the main part of extracted CGA. Hence, the capture of CGA from this side product would constitute an interesting valorization pathway. The aim of this work was to study CGA adsorption from the UF permeate on five macroporous resins including XAD4, XAD7, XAD16, XAD1180 and HP20 having various properties in term of polarity, pore diameters, specific area). On the resins exhibiting the best adsorption capacities, kinetics and isotherms experimental data were regressed at different temperatures in order to elucidate CGA adsorption mechanisms. Desorption by ethanol/ water mixtures was also investigated and the purity was considered in order to choose the most appropriate resin for CGA capture from this effluent.

MATERIALS AND METHODS

Chemical and reagents

The sunflower meal used was defatted by n-hexane at the industrial scale and provided by Saipol (Bassen, France). Chlorogenic acid (CGA, 5-O-caffeoylquinic acid), 4-O-caffeoylquinic acid (4-CQA), 3-O-caffeoylquinic acid (3-CQA) standards and the five macroporous resins (XAD7, XAD4, XAD16, XAD1180 and HP20) were purchased from Sigma-Aldrich (St. Louis, Missouri, USA). The characteristics of macroporous resins are shown in Table 1.

Resins	Material	Polarity	Specific surface (m²/g)	Pore (Å)
XAD4	SDVB*	Non polar	725	50
XAD7	Acrylate	Polar	450	90
XAD16	SDVB	Non polar	900	100
XAD1180	SDVB	Non polar	600	300
HP20	SDVB	Non polar	500	260

Table 1: Properties of XAD 7, XAD 16, XAD 4, XAD 1180 and HP 20

Sodium chloride (NaCl) and sodium hydroxide (NaOH) pellets were both from VWR (Darmstadt, Germany). Hydrochloric acid (HCl) solution was from Carlo Erba (Milan, Italy). Acetonitrile and formic acid at analytical grade were supplied by Fisher Scientific (Hampton, USA).

Sunflower protein extraction/purification process

The process was carried out in two stages as described in [27]. The first one was a solid/liquid extraction from the sunflower meal. The second was a protein purification by ultrafiltration (UF). The extraction step was achieved using a 0.5 M NaCl solution at a solid/liquid ratio of 1:9 (w/w). The pH of the slurry was adjusted at pH 7.5 with HCl 1 M and stirred at room temperature for 30 min. Then the slurry was centrifuged (Thermo Scientific Lynx 6000 centrifuge, USA) at 15000 g and 20°C for 30 min. The purification step was achieved with an Akta Flux 6 ultrafiltration apparatus (GE Healthcare Life Science, USA). The membrane used was a polyethersulfone hollow fiber membrane of 3 kDa cut-off (4800 cm² area, UFP-3, C-6A, GE Healthcare, USA). The transmembrane pressure was set at 1.5 bar and the feed rate at 1.5 L/min. In a first stage, six diavolumes (DV, DV = diafiltration solution volume/ initial volume) of 0.5 M NaCl solution was used to flush proteins from micro-solutes (low molar weight carbohydrate, minerals, non-protein nitrogen, and phenolic compounds). Then, NaCl was removed by three diavolumes of deionized water. The retentate compartment contained the purified proteins. The permeate obtained was collected and adjusted at pH 2 (in order to avoid phenol oxidation as recommended [28] and stored at -20°C before use.

Adsorption/ desorption study

Before each experiment, resins were washed with methanol for 10 minutes under magnetic stirring (150 rpm) at room temperature and rinsed with ultrapure water as recommended by the manufacturer. For each experiment, 1.5 g resin was mixed with 30 mL of permeate under magnetic stirring (150 rpm) at 25°C. After adsorption, resins were separated from the liquid phase by filtration (using Millex syringe Filter, PVDF, 0.22μm, non-sterile from ThermoFisher Scientific (USA). Liquid phases were analyzed by HPLC for phenolic compounds characterization and/ or CGA quantification.

Resin screenings

The resins were screened on the basis of massic (Eq. 1) and specific surface (Eq. 2) adsorption capacity :

The adsorption capacity (qe, amount of CGA adsorbed per g of resin, Eq. 1) was calculated as:

$$q_e = \frac{(C_0 - C_e)V_i}{W}$$

where Co and Ce are the initial and equilibrium concentrations of CGA in permeate solution respectively (mg/ mL); Vi is the initial volume of permeate added into the resins (mL); and W is the weight of the dried resin (g).

The specific surface adsorption capacity (SA, amount of CGA per m² of resin, equation 2) was calculated as:

$$SA = \frac{(C_0 - C_e)V_i}{SS \times W}$$

where SA is the surface adsorption capacity (mg / m2), SS is the resin specific surface (m²/ g).

Adsorption kinetics

Adsorption capacity was monitored after 5, 10, 15, 30, 60, 90, and 120 min. To do so, CGA concentration was measured in the liquid phase by HPLC. From the concentration, qe and/ or SA was deduced. Results were plotted under linearized models (pseudo-first-order, pseudo-second-order, and intra-particle diffusion, Table 2).

Kinetic model	Linear form	Plot	Parameter	Resin	
				XAD 7	XAD 16
Pseudo-first-order	$\ln(q_e - q_t) = \ln q_e - k_1 t$	$\ln(q_e - q_t)$ $vs\ .t$	$k_1(1/min)$	-0.082	.053
			$q_{e.exp}(mg/m^2)$	Pseudo-second-order	0.017
			$q_{e.cal}(mg/m^2)$	0.016	0.01
			R^2	0.971	0.982
Pseudo-second-order	$\dfrac{1}{q_t} = \dfrac{1}{k_2 q_e^2} + \dfrac{t}{q_e}$	$\dfrac{1}{q_t}\ vs.\ t$	$k_2\ (m^2/(mg.min)$	0.036	0.057
			$q_{e.exp}(mg/m^2)$	0.0273	0.017
			$q_{e.cal}(mg/m^2)$	0.0274	0.017
			R^2	0.9999	1
Intra-particle diffusion	$q_t = kt^{\frac{1}{2}} + C$	$q_t\ vs.t^{\frac{1}{2}}$	$K_{i,1}(m^2.mg^{-1}.min^{-1/2})$	0.0024	0.0017
			$C_1(mg/m^2)$	0.014	0.0074
			R^2	0.9829	0.9848
			$K_{i,2}(m^2.mg^{-1}.min^{-1/2})$	0	0
			$C_2(mg/m^2)$	0.027	0.016

Table 2: Equations and parameters for the adsorption kinetic models of CGA obtained with the XAD7 and XAD16 resins.

Adsorption isotherms

Adsorption isotherms expressed the relationship between CGA adsorption capacity (qe, mg/g) and the concentration of sample solution in the liquid phase at the equilibrium (Ce, mg/ L). For the adsorption study, a duration of 120 min was chosen. Experiments were carried out at 25°C (298.15 K). Langmuir and Freundlich models were used to regress experimental data (Table 3).

Isotherm model	Non-linear form	Parameter	Constraint	Resin	
				XAD 7	XAD 16
Langmuir	$q_e = \dfrac{Q_{max} K_L C_e}{1 + K_L C_e}$	$Q_{max}(mg/m^2)$ $K_L(L/mg)$ R^2	$q_e = \dfrac{Q_{max} K_L C_e}{1 + K_L C_e}$	0.054 0.026 0.9899	0.040 0.021 0.9586
Freundlich	$q_e = K_F C_e^n$	$K_F\left(\dfrac{mg}{m^2}\right)/\left(\dfrac{mg}{L}\right)^n$ n R^2	$0 < n \le 1$	0.007 0.358 0.8690	0.003 0.445 0.9119

Table 3: Adsorption isotherm models and parameters for the phenolic compound obtained with the two resins selected XAD7 and XAD16.

Adsorption thermodynamic parameters

The effect of the adsorption temperature was investigated by determining the adsorption isotherms at 298.15, 308.15, and 318.15 K. Enthalpy and entropy variations were obtained from the slope and intercept of the linear plot lnKeq vs 1/T according to the linear form of Clausius-Clapeyron Eq. 3:

$$ln\ Keq = -\frac{\Delta H}{RT} + \frac{\Delta S}{R}$$

where lnKeq is the natural logarithm of the constant of adsorption equilibrium (Keq), ΔH is the enthalpy change (J/ mol), ΔS is entropy change (J/ mol), R is the universal gas constant (8.3144 J/(molK) and T is the absolute temperature in Kelvin (K).

ΔG was determined using Eq. 4:

$$\Delta G = -\ RT\ ln\ Keq \qquad (4)$$

where ΔG (J/ mol) is the Gibbs energy change.

Desorption

Desorption ratio were determined using different water/ethanol solvents after the adsorption step on XAD7 and XAD16 up to equilibrium. To do so, 40 mL of 30, 50, 70, and 90%, v/v was added to the resins, and shaken at 150 rpm at 25°C for 2 hours (to reach desorption equilibrium). Resins were washed with deionized water twice prior solvent addition. Resins were separated from the liquid filtration using filter paper. CGA concentration in the liquid was quantified by HPLC. Desorption ratio was calculated using Eq.5:

$$Desorption\ ratio\ (\%) = \frac{C_d V_d}{(C_o - C_e)V_i}100\%(5)$$

where Cd is the concentration of CGA in desorption solution (mg/ mL), Vd is the volume of the desorption solution (mL).

The purity of CGA after desorption step was determined using Eq.6:

$$Purity\ of\ CGA\ (\%) = \frac{Amount\ of\ CGA\ after\ desorption\ (mg)}{Total\ total\ mass\ (mg)}100\%(6)$$

Analytical methods

CGA identification and quantification

CGA concentration in the liquid by-product was quantified by HPLC (Shimadzu Corporation, Kyoto, Japan) according to [27] with some modification. The equipment used included a pump with a degasser (LC-20AD), an auto-sampler (SIL-20AC), a column oven (CTO-20A), a diode array detector (CPO-M20A) and a LCSolutions software. The analysis was carried out with a Biosep SEC-s2000 column (300 x 7.8 mm, 5 µm) purchased from Phenomenex (Torrance, CA, USA). The mobile phase consisted of formic acid: ultrapure water: acetonitrile mixture (0.1%: 55%: 45%, v/v). The injection volume was 5 µL. The flow rate was 0.6 mL/min. The detection wavelength was 325 nm. The oven temperature was kept at 35°C. All solutions and samples were filtered through 0.45 µm membranes (Fisher Scientific, Hampton, USA) before injection. CGA identification was done from standards retention time by on-line electrospray ionization mass spectrometry (ESI-MS). Data acquisition and processing were monitored with LabSolution software (Shimadzu Corporation, Kyoto, Japan). Nitrogen was used as drying gas at a flow rate of 21.5 L/ min. The nebulizer temperature was set at 300°C. CGA was searched in positive mode at m/z = 355.3+. A CGA calibration curve with concentrations ranging from 0.05 to 1.25 mg/mL was used for the quantification (linear regression equation was y = 25057208.61x with R^2 = 0.9983).

NaCl content

NaCl content in the permeate was assessed by conductimetry (Meterlab PHM 210, Radiometer analytical, France). The quantification was done using an NaCl calibration curve ranging from 0.2 to 50 g/L (y = 1.9054x with R^2 = 0.9908).

Total carbohydrate content

Total carbohydrate content in the permeate was measured by the method of anthrone-sulfuric acid presented by Yemm and Willis with some modifications [29]. Briefly, samples were mixed with 2 g/L anthrone in 98% sulfuric acid in boiling water for 10 min. After cooling, the absorbance of the solution was measured at 620 nm in a multiplate (Multiskan GO, Thermo scientific, Japan). Glucose was used as standard with concentration ranging from 0.1 to 1 mg/ mL (y = 1.1845x, R^2 = 0.9981).

Nonprotein nitrogen content

Kjeldahl method was used to measure the total nitrogen in the permeate [30]. A nitrogen-to-protein conversion coefficient of 5.6 was applied as recommended in [27] for sunflower source.

Dry matter

1 mL of permeate was put in aluminium dish and left in oven during 24 h at 111°C. Afterward, aluminium dish was weighted regularly until reaching a constant weight.

Data analysis

All experiments and analytical measurements were carried out three times. Data displayed corresponded to the average value with the standard deviation. Statistical analysis was performed by Student's t-test with Rstudio 3.6.1 (Boston, MA, USA). A p-value inferior to 0.05 was considered a significant difference. All figures were designed by OriginPro 8.5 package (MA, USA). The chemical structures of phenolic compounds and CGA interaction forces with selected resins were illustrated using ChemDrawUltra 8.0 software (Cambridge Soft, MA, USA).

RESULTS AND DISCUSSION

Characterization of the ultrafiltration permeate from sunflower protein purification

Figure 1 shows the SE-HPLC chromatogram at 325 nm and 280 nm of ultrafiltration (UF) permeate obtained from the purification of proteins extracted from sunflower meal at pH 7.5, 0.5 M NaCl. This figure shows the main peak at 32 min of retention time. Marginal signals can be observed at 13, 37 and 39 min of retention time. The first minor peak (13 min) corresponded to the column void volume and showed a higher signal at 280 nm rather than 325 nm. SDS-PAGE analysis of this peak revealed the presence of proteins in a molar weight range of sunflower albumins (SFA, 10-18 kDa) [27]. Hence, the 3 kDa membrane used for the purification probably allowed the transmission of traces of these proteins. SFA is particularly associated with phenolic compounds by covalent bonds [31]. This would explain the signal observed at 325 nm at this retention time. Peaks at 32, 37, and 39 min revealed the presence of molecules with m/z of 355 in positive mode ESI-MS. This corresponds to chlorogenic acid (CGA) m/z. The figure also shows that standard CGA isomers had the same retention times (5-CQA at 32 min, 3-CQA at 37 min, and 4-CQA at 39 min). This indicated that free polyphenolic fraction in the UF permeate was composed of CGA, mainly in its 5-CQA isomer. The predominance of CGA in sunflower and relative in aqueous extracts of sunflower meal [13,27]. The relative absence of caffeic acid and CGA dimers that account for 15-20% of total phenolic compounds in the meal according to Weisz GM et al. 2009 [13] are probably less extracted in aqueous solvents due to their polarity lower than CGA. In any cases, it makes this side products of sunflower meal protein purification a particularly attractive source of CGA. Indeed, generally recognized
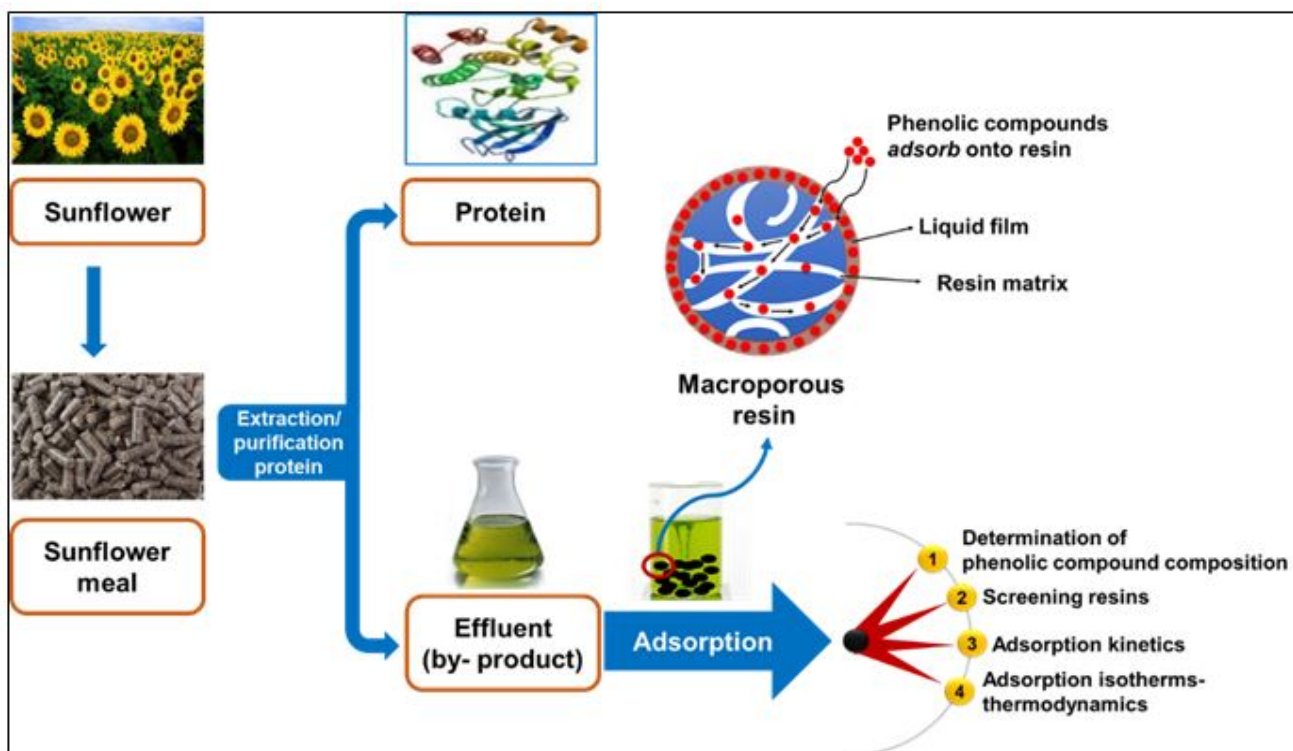
Graphical abstract: Scheme-Illustration of phenolic compounds adsorption from an aqueous by-product of sunflower protein extraction.
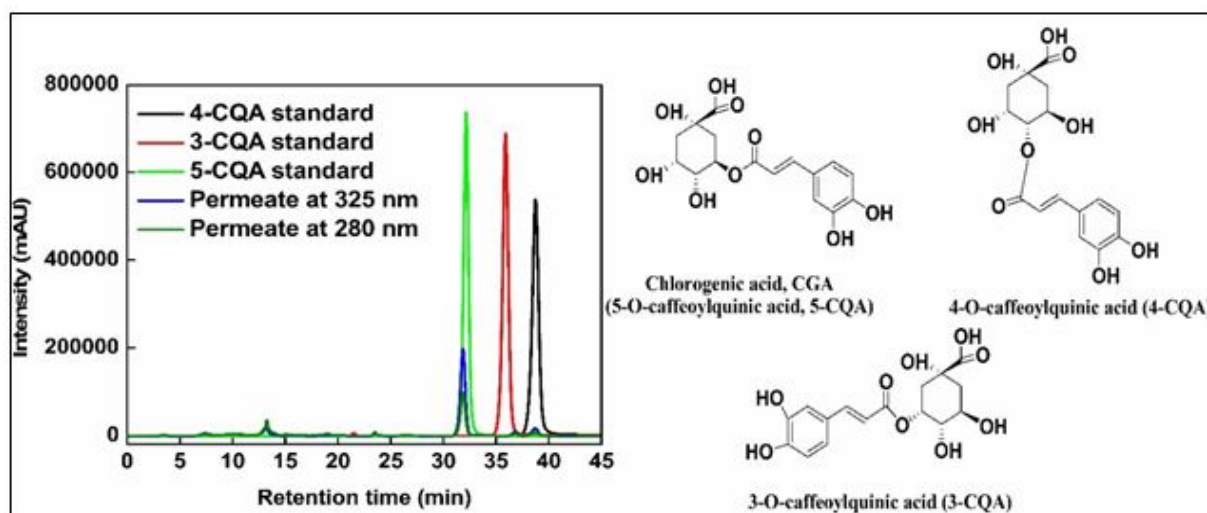

Figure 1: SE-HPLC chromatogram and structures of phenolic compounds detected in the UF permeate obtained from sunflower protein purification. Chromatograms were recorded at 325 and 280 nm. The elution of CGA isomers in the same conditions was also displayed.

as interesting sources of CGA like low-grade coffee bean, coffee bean methanol extracts or Crafton weed ethanol extracts are composed of many other phenolic compounds [6,32,33].

Component	Compound	Proportion (%)
Liquid by-product(UF permeate)	Chlorogenic acid, CGA (5-CQA) % dm	1.13 ± 0.21
	NaCl % dm	87.67 ± 11.93
	Total carbohydrates % dm	3.53 ± 1.98
	Nitrogen contain-ing molecules (N x 5.6) % dm	0.11 ± 0.02
	Ash % dm	7.56 ± 0.70

Table 4: Composition of the liquid by-product.

Table 4 presents the proximate composition of the permeate dry matter. The high content in NaCl (87 ± 11.93 %) was consistent with a large amount of NaCl either for the protein extraction step and the protein purification. Ash (7.56 ± 0.70%) were minerals extracted from the meal that also highly crossed the membrane. The permeate also contained carbohydrates (3.53 ± 1.98%). These were probably soluble fibers with molar weights low enough to cross the membrane or simple carbohydrates (both contained in the sunflower meal [34]). The nitrogen-containing biomolecules fraction (0.11 ± 0.02 %) is probably not homogeneous. A part of it might be the albumin traces in the permeate. Besides, about 11% of nitrogen assayed by Kjeldahl analysis in the protein extract remained soluble in 10% (v/v) trichloro acitic acid (TCA) (data not shown). These nitrogen containing molecules are classically referred to as 'non-protein' nitrogen and meant to be low molar weight peptides, free amino acids and/ or nucleic acids. These molecules probably constituted the other part of the nitrogen containing molecules observed.

This table also shows that around 25% of the UF permeate organic dry matter is composed of CQA. The rest of the organic matter is composed of polar molecules. Liu B et al. 2016 [6] showed that polar resin exhibited higher CGA adsorption capacity than apolar or mildly polar ones. But they observed poor CGA purity after desorption step. This was due to the competitive adsorption of polar molecules on the polar resin. Or it is likely that polarity and affinity characteristic of the elution solution and the adsorbed components may influence the purity of CGA. Hence, for CGA capture from sunflower meal aqueous extract, apolar or mildly polar resin should be more appropriate.
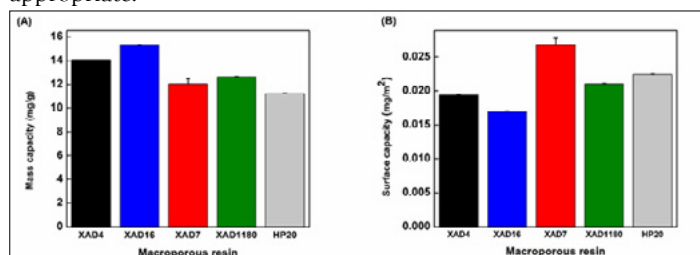

Figure 2: Mass (A) and surface (B) adsorption capacity of CGA on XAD4, XAD16, XAD7, XAD1180, and HP20.

Figure 2A shows CGA adsorption capacity from XAD4, XAD7, XAD16, XAD1180, and HP20. Those resins were known for their ability to adsorb phenolic compounds from many different plant extract [35,36]. XAD16, XAD4, XAD1189, and HP20 were apolar

resins made of styrene divinylbenzene (SDVB). XAD7 was a slightly polar resin made of an acrylic polymer.

XAD16 and XAD4 showed the highest adsorption capacity at equilibrium (15.32 ± 0.04 mg/g and 14.07 ± 0.01 mg/g respectively). XAD7, XAD1180 and HP20 had lower values (12.03 ± 0.45, 12.62 ± 0.07 and 11.21 ± 0.02 mg/g dried resin, respectively). The very similar CGA adsorption capacity was observed with XAD7 and HP20 (11 mg/g and 15 mg/g, respectively) from crafton weed extract [6]. Besides, XAD16 was shown to be particularly efficient for CGA adsorption from sunflower meal aqueous extracts [25,26]. The adsorption capacity depends on adsorption kinetics pattern, molecule affinity toward the material and resin specific area [37]. It can also be modulated by the pore diameter. Indeed, if the diameter is low enough (≤ 50 Å) it can induce diffusional limitations by steric hindrance [35,37] or even limit the accessibility of a fraction of the resin area.

Table 1 shows material, pore diameters, and specific area of the resins used in the study. Non-polar resins, Among SDVB resins, XAD16 showed the highest specific area (900 m²/g) followed by XAD4, XAD1180, and HP20. Interestingly, this ranking corresponded to the observed capacity values. XAD4 had the smallest pore diameters (50 Å). This indicated that SDVB resin mass capacities were essentially governed by the contact area. Probably no or few diffusional limitations due to the pore size occurred [38]. This was also suggested by Liu B et al. 2016 [6] with CGA capture from Eupatorium Adenophlorium extracts.

In order to investigate the effect of a resin material on CGA adsorption, surface capacity had to be compared. Figure 2B shows that XAD7 had by far the highest surface capacity (27 µg/m² dry resin) whereas its specific area was rather low (450 m²/g). For SDVB resins the value was close to 20 µg/m2). This indicated that acrylic material had a better affinity than SDVB toward CGA.
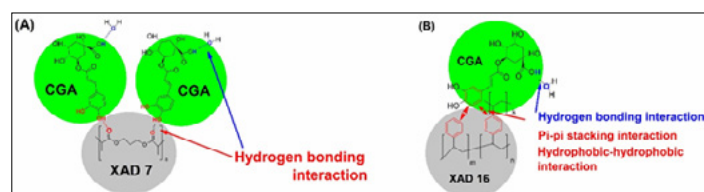

Figure 3: Schemes for mechanism proposed of the adsorption process of the phenolic compound onto the different resins. (A) CGA onto XAD7 resin and (B) CGA onto XAD16 resin.

Lin L et al. 2012 [39] reported that chemical features of XAD7 and HP20 resins were as important as physical characteristics on phenolic compounds adsorption [39]. The adsorption mechanism remains unclear though. In this study, we propose a possible CGA interaction scheme with acrylic and SDVB resins (Figure 3). CGA would interact with XAD7 through hydrogen bonding implying alcohol functions of the caffeic acid part and the acrylate ester bonds of the resin backbone. Hydrophobic interactions between the caffeic part (benzene ring) and acrylate carbon backbone might also take place (Figure 3B). Water molecules are probably partly excluded from this backbone, otherwise, they would compete with CGA and no CGA adsorption would occur. It is more likely that the highly hydrophilic quinic acid part interacts more favorably with the bulk water molecules.

In a different way, the interaction of CGA – SDVB resins should rather be through ᴨ stacking interactions. The highest efficiency of acrylate material to capture CGA could be due to the highest amount of binding sites. But the very high specific area of XAD16 makes it the better resin in terms of massic capacity.

The adsorption kinetics, isotherms, thermodynamics properties, and CGA desorption were further investigated with XAD7 and XAD16 to better understand the process with these two resins.
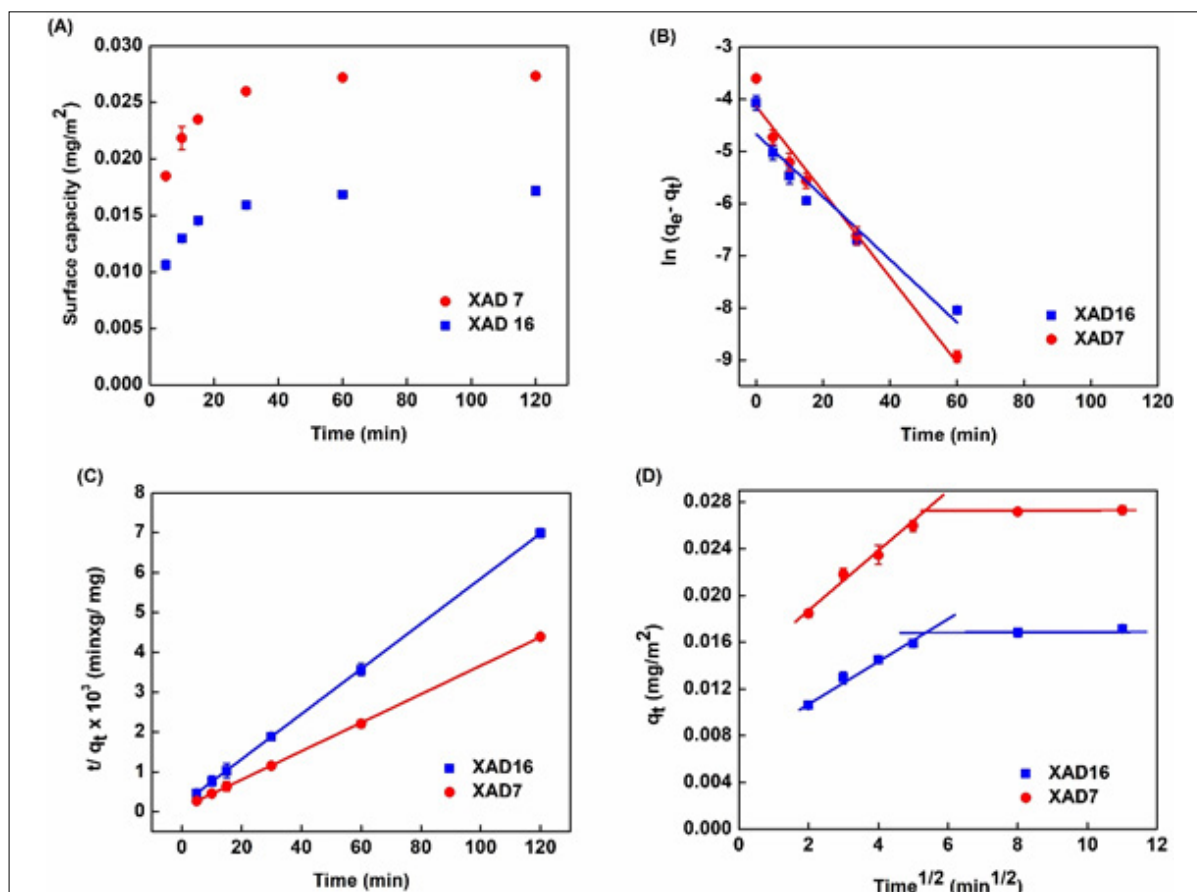
Adsorption kinetics

Figure 4: Adsorption kinetics of CGA with XAD 7 and XAD 16. (A) surface adsorption kinetic curves, (B) pseudo-first-order model, (C) pseudo-second-order model, and (D) intra-particle diffusion model (in linearized forms).

Adsorption kinetics of CGA (from UF permeate) on XAD7 and XAD16 were presented in Figure 4A. Very similar trends were observed with the two resins. A large part of CGA was quickly adsorbed (up to 80% of the equilibrium capacity in 15 min). Then the adsorption kinetics slowed down and the equilibrium happened between 60 min and 120 min. Thus, the adsorption process should be conducted for 120 min to achieve an equilibrium state. Interestingly, Liu B et al. 2016 [6] observed that CGA adsorption equilibrium with a highly polar resin (NKA – II) was reached at 300 min. This resin had an average pore size similar to XAD7 and XAD16 (around 120 Å). So the adsorption process on apolar or slightly polar resin would be quicker.

Adsorption kinetics were regressed with pseudo-first-order (PFO, [40]) and pseudo-second-order (PSO, [41]) equations in the linearized form (Figure 4B-C). Table 2 shows the corresponding equations, parameter values of the models, and R2 of the linear regressions. The R2 obtained with linearized PFO (ln(qe-qt) vs. t) was less than 0.98. Furthermore, the calculated qe for XAD7 (0.016 mg/m²) and XAD16 (0.010 mg/m²) was found very different from experimental values (0.027 mg/m² for XAD7 and 0.017 mg/m² for XAD16). On the other hand, R2 of the linear regression of the t/qt vs t plot was very close or equal to 1 (0.999 and 1 for XAD7 and XAD16, respectively). Moreover, the calculated qe (0.0274 mg/m² for XAD7 and 0.017 mg/m² for XAD16) predicted from PSO model was very near the experimental values of qe (0.0273 mg/m² for XAD7 and 0.017 mg/m² for XAD16). These results indicate that adsorption kinetics followed a PSO model for the two resins. This was also observed with adsorption of CGA from Eupatorium adenophorum Spreng extracts on NKA-II resin [6] and Helianthus tuberosus L. leaves extracts on ADS-21 resin [20].

Solute transport phenomena are complex in adsorption processes. In the liquid phase, solutes are transported by convection and diffusion. There is also a diffusive transport from the liquid phase to the bead surface (through a limit liquid film) and a diffusive transport inside the particle pores. Adsorption kinetics may be modulated by several diffusional types of transports. The intra-particle diffusion model [42] is commonly used to investigate the diffusive rate-controlling phenomenon [43-45].

Figure 4D shows qt vs t1/2 plots obtained with XAD 7 and XAD 16. These plots correspond to the linear form of the intra-particle diffusion model (Table 2). For both the two resins, a linear evolution with two slopes is observed. The slopes represent the constant rate (ki) of each adsorption step while Ci (intercept at y-axis) is related to the thickness of the limiting layer. R2, ki, and Ci values obtained from linear regressions are displayed in Table 2. In the two cases, k1 (0.0024 and 0.0017 m²/(mgmin0.5) for XAD7 and XAD16, respectively) are by far higher than k2 (approximately 0) for the two resins. It can also be noticed that R² values for XAD7 and XAD16 are 0.9829 and 0.9848, respectively. This indicates that for both the two resins the adsorption process is limited by two diffusional effects. Very similar results were observed with the adsorption of alfalfa phenolic compounds and on HP20 and AER1 resins [44]. It was interpreted as a two steps adsorption process. The first one is related to the diffusional transport throughout the boundary layer at the liquid/ beads interface. Its high rate constant (Ki,1 was 0.0024 and 0.0017 (mg/m²) for XAD7 and XAD16, respectively) indicates a low diffusional limitation. The second one is due to intraparticle diffusion. The low rate constant (Ki,2 approximately equal to 0 for both resins) associated indicates a strong diffusional limitation. Such observation and explanation were also made by others [36,46,47]. Curiously, it can be noticed that the first step involved the adsorption of the largest part of the phenolic compounds (more than 90% of the adsorption at the equilibrium). This tends to indicate that the intraparticle diffusion limitation

only took place for a small part of phenols adsorption. Since the intraparticle diffusion happens inside bead pores, representing the largest part of the resin surface it can be hypothesized that the limitation only concerns the deepest zone of the pores. The diffusion inside pores near the surface is probably only limited by the boundary layer. This would explain why the intraparticle diffusion limitation affects less than 10% of the overall adsorption. The close pore size of the two resins (around 100 Å) explains their close behavior in terms of diffusional limitations.
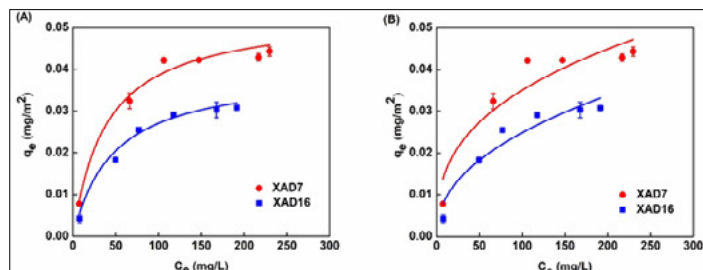
Adsorption isotherms

Figure 5: Adsorption isotherms non-linear fitting of selected XAD 7 and XAD 16 resin. (A) Langmuir model and (B) Freundlich isotherm model.

Figure 5 shows the adsorption isotherms of CGA on XAD7 and XAD16 at 25°C. Data were regressed with Langmuir (Figure 5A) and Freundlich (Figure 5B) equations as commonly done elsewhere [6,20,26]. Table 3 listed the R^2 of the regression, equations, and model parameters with XAD7 and XAD16. R2 values indicated that experimental data were better fitted by the Langmuir model (0.9899 and 0.9586 for both XAD7 and XAD16, respectively) than the Freundlich model (0.8690 and 0.9119 for XAD and XAD16, respectively). This indicated that the adsorption mechanism was the same for the two studied resins. It consisted in a monolayer adsorption of phenolic compounds at the surface resin [6,20,26]. These findings also are in agreement with other work on CGA adsorption on XAD16 HP and NKA-II resins from other sources [6,26].

Table 3 indicated that maximum adsorption capacity based on the resin area of XAD7 was higher than XAD16 (0.054 mg/m² vs. 0.040 mg/m2). However, as expected from screening experiments, XAD16 showed higher maximum capacity when results were based on resin amount (36.59 mg/g for XAD16 vs. 26.21 mg/g for XAD7). Considering kinetics result with the two resins it can be deduced that XAD7 polymer (acrylate resin) had a better adsorption property than XAD16 polymer (styrene divinyl benzene). The far better specific surface area of XAD16 (900 m²/g vs. 450 m²/g) probably made its highest massic adsorption capacity. In any case, it would confirm the hypothesis of a higher adsorption site density on acrylate material.

Besides, Qmax value of CGA adsorption from a sunflower (Helianthus annuus L.) aqueous extract on XAD16HP was observed at 42.7 mg/g [25]. This result is close to what is observed here. The discrepancy may be due to the interference of other organic molecules. Indeed, the above-mentioned article dealt with a raw extract containing proteins. It might also be due to the impact of an ionic strength. In this study a UF permeate was used (vs. a whole extract) and the NaCl content was around 0.5 M. Qmax observed here were lower than on the highly polar NKA-II resin (66.863 mg/g) [6]. Authors claimed that this high adsorption capacity was due to the resin polarity, but discrepancies are harder to interpret since the starting material was different (Crofton weed extract).
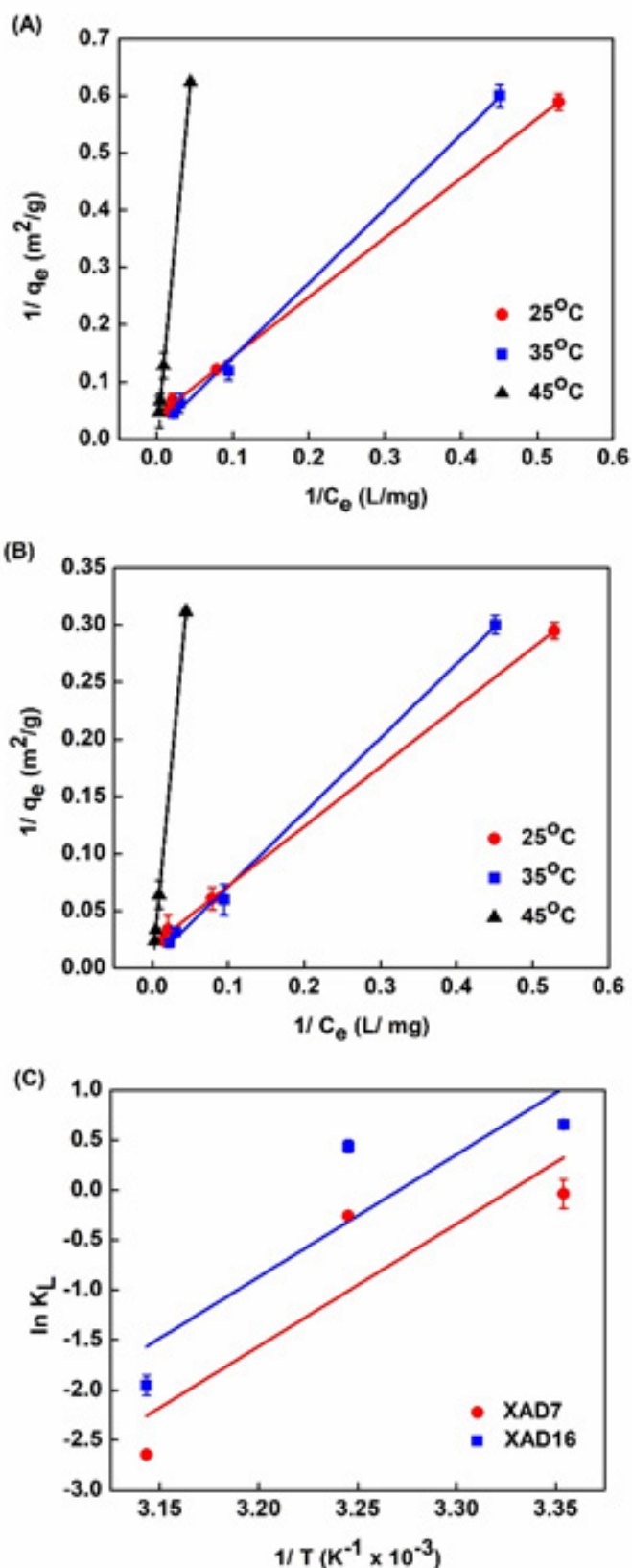
Determination of thermodynamic parameters

Figure 6: Equilibrium adsorption isotherm using the Langmuir model in linear form. (A) XAD7 and (B) XAD16 at 25°C, 35°C and 45°C; (C) ln KL vs. 1/T plot of adsorption equilibrium constant KL using the Langmuir model.

The effect of temperature on both resins adsorption capacity of

Resin	Temperature (0C/ K)	Isotherm parameter			Thermodynamic parameter		
		Langmuir model					
		KL	Qmax(mg/m²)	R2	ΔH (kJ/mol)	ΔG(kJ/mol K)	ΔS (kJ/mol K)
XAD7	25/298.15	1.923	0.13	0.9945	-37.75	-2.235	-0.119
	35/308.15	1.543	0.12	0.9994		-1.044	
	45/318.15	0.142	0.09	0.9998		0.147	
XAD16	25/298.15	1.923	0.19	0.9994	-22.47	-1.932	-0.068
	35/308.15	1.543	0.09	0.9982		-1.243	
	45/318.15	0.142	0.07	0.9997			

Table 5: Isotherm and thermodynamic parameters of phenolic compound adsorption on XAD 7 and XAD 16 at 25°C, 35°C and 45°C.

CGA was also investigated in order to get the thermodynamic parameters of adsorption. Figure 6A-B shows adsorption isotherms at 25°C, 35°C and 45°C (linearized Langmuir model). Langmuir model parameters and R² were listed in Table 5. Obviously, the adsorption of phenolic compounds decreased with increasing temperature (Table 5). XAD7 Qmax ranged from 0.13, to 0.09 mg/m² from 25°C to 45°C while XAD16 Qmax value decreased from 0.19, 0.09 and 0.07 mg/m² in the same temperature range. ΔH and ΔS were determined through the slope and intercept of ln KL against 1/T (Eq. 3) (Figure 6C) according to Van Hoff's equation. The enthalpy changes (ΔH) for the CGA adsorption process on both XAD7 and XAD16 resin were -37.35 and -22.47 kJ/mol, respectively (Table 5). Negative values indicate an exothermic adsorption process. The fact that values were less than 43 kJ/ mol demonstrated that the adsorption process of CGA on the resins was governed by physical rather than chemical interactions [35,48,49]. That demonstrated that XAD7 and XAD16 resins would not undergo structural changes during the CGA adsorption process. Therefore, adsorption of CGA on the resins only takes place through physical mechanism with no chemical reactions. This observation was also reported in the work of Gao ZP et al. 2013 [50] when they studied the adsorption of polyphenols separation from kiwifruit juice using AB-8 resin [50]. Furthermore, it indicated that the adsorption process of CGA for both resins should be conducted at room temperature (around 25°C). In addition, the entropy changes (ΔS) values of XAD7 and XAD16 were -0.119 and -0.068 kJ/molK, respectively. These negative values suggested a random adsorption process at the solid-liquid interface [51] which happened owing to the desorption process of water molecules previously adsorbed onto the resins' surface [50]. The negative free energy change (ΔG) deduced from ΔH and ΔS (Table 4). suggested that CGA adsorption onto XAD7 and XAD16 was a spontaneous process. Moreover, the absolute value of ΔG < 20 kJ/mol confirmed physical adsorption of CGA onto both resin [50,52]. These results are also online with the proposed adsorption scheme in Figure 3.

Desorption of CGA on XAD7 and XAD16

Ethanol solutions from 30, 50, 70, and 90%, v/v were used to desorb CGA from XAD7 and XAD16. Desorption kinetics showed that 120 min was necessary to reach the equilibrium (data not shown). This observation was in agreement with Xi L et al. 2015 [53] that studied the desorption static of polyphenols from sweet potato Ipomoea batatas L. leaves on AB-8 resin. Figure 7 shows a maximum of CGA desorption ratio from 70% ethanol (v/v) in both the two cases. At this ethanol concentration (and higher), the desorption ratio was around 90%. Xi L et al. 2015 [53] also

showed that the highest desorption ratio (90.9%) was observed when ethanol concentration was 70% (v/v). Such a maximum ratio was also observed with the desorption of flavonoids from G. glabra L. leaf from XAD16 (at ethanol 80%, v/v) [36]. Interestingly, for ethanol concentration below 70% (v/v), the desorption ratio of CGA for XAD16 was higher than for XAD7 (p < 0.05). Relatively large desorption ratio discrepancies were particularly observed at 30% ethanol (48.08% for XAD7 and 56.03% for XAD16). This may indicate stronger interactions throughout hydrogen bonding (occurring with XAD7) rather than ⱶ - ⱶ interactions (occurring with XAD16). In the past, Liu B et al. 2016 [6] reported that the purity of CGA from the organic extract of Eupatorium adenophorum Spreng was 22.17% using NKA-II macroporous resin (polar). Meanwhile, Sun PC et al. 2015 [20] indicated that CGA separation from Helianthus tuberosus L. leaves extract by ADS-21 (polar resin) was 65.2%. On the contrary, in this study, the purity of CGA from sunflower meal when we used XAD7 and XAD16 were 77.56 ± 0.99 and 74.59 ± 0.12%, respectively. It might be the effect of the polarity of macroporous resin on the adsorption selectivity of CGA to some degree. The results in the current study indicated that selected macroporous resins were efficient for separation of CGA notably with XAD7 resin (moderate polar resin).

CONCLUSION

XAD7 (mildly polar) and XAD16 (apolar) showed high CGA surface and massic adsorption capacities (from an aqueous by-product of sunflower protein purification process). The adsorption kinetics of polyphenols on the two resins followed a pseudo-second-order model with a similar intraparticle diffusion pattern. The Langmuir model described more accurately the adsorption behavior of phenolic compounds on both the two resins indicating a monolayer adsorption behavior. The negative value of enthalpy, entropy, and Gibbs free energy indicated spontaneous and exothermic processes. Hence, the adsorption process was controlled by a physical mechanism and should be favorably performed at low temperatures. We concluded that the high surface adsorption capacity on XAD 7 was probably due to a high frequency of the binding sites on acrylate polymer. The high massic adsorption capacity observed with XAD16 is due to its very high specific area. In addition, the highest desorption ratio was observed at ethanol solution at 70% (v/v) but slight discrepancies were observed between the two resins. This would be due to the different interactions at stake between CGA and the two resins (hydrogen bond with XAD7 and ⱶ – ⱶ stacking with XAD16).

CONFLICT OF INTEREST

The authors declare that they have no conflict of interest.

LIST OF ABBREVIATION/ NOMENCLATURE

SFA   Sunflower Albumin

DF   Diafiltration

UF   Ultrafiltration

TCA   Trichloro acetic acid

SE-HPLC Size exclusion high-performance liquid chromatography

SDS-PAGE Sodium dodecyl sulfate – polyacrylamide gel electrophoresis

PVDF   Polyvinylidene diflouride

CGA   chlorogenic acid

3-CQA   3-O-caffeoylquinic acid

4-CQA   4-O-caffeoylquinic acid

5-CQA   5-O-caffeoylquinic acid

q_e adsorption capacity (mg/g)

C_0 initial concentration of phenolic compound (mg/mL)

V_i volume of the initial sample solution (mL)

W   weight of the tested dry resin (g)

C_e equilibrium concentration of phenolic compound (mg/mL)

SA   surface adsorption capacity (mg / m2)

SS   specific surface (m2/ g)

PFO   pseudo-first-order

PSO   pseudo-second-order

q_t amount of adsorbate uptake per mass of adsorbent at any time t (min)

k_1 rate constant of the PFO equation (1/min);

k_2 rate constant of the PSO equation(g/mg×min)

k_i rate constant of the intra-particle diffusion model (mg/$gmin^{1/2}$)

C   constant associated with the thickness of the boundary layer (mg/g)

Q_{max} maximum saturated monolayer adsorption capacity of polyphenol (mg/g)

K_L Langmuir constant (L/mg)

K_F Freundlich constant (mg/g)/(mg/L)^n

n   Freundlich intensity parameter ($0 < n \leq 1$)

ΔH enthalpy change (kJ/mol)

ΔS entropy change (kJ/mol K)

ΔG Gibbs free energy change (kJ/ mol K)

R   ideal gas constant (8.314 J/ mol K)

T   temperature (K)

Keq   equilibrium distribution coefficient of adsorption isotherm

REFERENCES

1. Wong SK, Chin KY, Suhaimi FH, Ahmad F, Ima-Nirwana S. Effects of metabolic syndrome on bone mineral density, histomorphometry and remodelling markers in male rats. PLoS ONE. 2018;13(2):e0192416.

2. Ren J, Zheng Y, Lin Z, Han X, Liao W. Macroporous resin purification and characterization of flavonoids from Platycladus orientalis (L.) Franco and their effects on macrophage inflammatory response. Food Funct. 2017;8(1):86-95.

3. Zhang H, Tsao R. Dietary polyphenols, oxidative stress and antioxidant and anti-inflammatory effects. Curr Opin Food Sci. 2016;8:33-42.

4. Tajik N, Tajik M, Mack I, Enck P. The potential effects of chlorogenic acid, the main phenolic components in coffee, on health: a comprehensive review of the literature. Eur J Nutr. 2017;56(7):2215-2244.

5. Li P, Huo L, Su W, Lu R, Deng C, Liu L, et al. Free radical-scavenging capacity, antioxidant activity and phenolic content of Pouzolzia zeylanica. J Serb Chem Soc. 2011;76(5):709-717.

6. Liu B, Dong B, Yuan X, Kuang Q, Zhao Q, Yang M, et al. Enrichment and separation of chlorogenic acid from the extract of Eupatorium adenophorum Spreng by macroporous resin. J Chromatogr B. 2016;1008:58-64.

7. Tan Z, Wang C, Yi Y, Wang H, Li M, Zhou W, et al. Extraction and purification of chlorogenic acid from ramie (Boehmeria nivea L. Gaud) leaf using an ethanol/salt aqueous two-phase system. Sep Purif Technol. 2014;132:396-400.

8. http://www.fao.org/faostat/en/#data/QC/visualize (accessed on 26th May 2020), (n.d.).

9. Geneau-Sbartai C, Leyris J, Silvestre F, Rigal L. Sunflower Cake as a Natural Composite: Composition and Plastic Properties. J Agric Food Chem. 2008;56(23):11198-11208.

10. Pickardt C, Weisz GM, Eisner P, Kammerer DR, Neidhart S, Carle R. Processing of low polyphenol protein isolates from residues of sunflower seed oil production. Procedia Food Sci. 2011;1:1417-1424.

11. Canella M, Sodini G. Extraction of gossypol and oligosaccharides from oilseed meals. J Food Sci. 1977;42(5):1218-1219.

12. Sripad G, Rao MN. Effect of methods to remove polyphenols from sunflower meal on the physicochemical properties of the proteins, J Agric Food Chem. 1987;35(6):962-967.

13. Weisz GM, Kammerer DR, Carle R. Identification and quantification of phenolic compounds from sunflower (Helianthus annuus L.) kernels and shells by HPLC-DAD/ESI-MSn. Food Chemistry. 2009;115:758-765.

14. Ky CL, Noirot M, Hamon S. Comparison of Five Purification Methods for Chlorogenic Acids in Green Coffee Beans (Coffea sp.). J Agric Food Chem. 1997;45:786-790.

15. Conidi C, Cassano A, Caiazzo F, Drioli E. Separation and purification of phenolic compounds from pomegranate juice by ultrafiltration and nanofiltration membranes. J Food Eng. 195 (2017) 1–13.

16. Zagklis DP, Vavouraki AI, Kornaros ME, Paraskeva CA. Purification of olive mill wastewater phenols through membrane filtration and resin adsorption/desorption. J Hazard Mater. 2015;285:69-76.

17. Jia G, Lu X. Enrichment and purification of madecassoside and asiaticoside from Centella asiatica extracts with macroporous resins. J Chromatogr A. 2008;1193:136-141.

18. Liu QS, Zheng T, Wang P, Jiang JP, Li N. Adsorption isotherm, kinetic and mechanism studies of some substituted phenols on activated carbon fibers. Chem Eng J. 2010;157(2-3):348-356.

19. Scordino M, Di Mauro A, Passerini A, Maccarone E. Adsorption of Flavonoids on Resins: Hesperidin. J Agric Food Chem. 2003;51:6998-7004.

20. Sun PC, Liu Y, Yi YT, Li HJ, Fan P, Xia CH. Preliminary enrichment and separation of chlorogenic acid from Helianthus tuberosus L. leaves extract by macroporous resins. Food Chemistry. 2015;168:55-62.

21. Gonzalez Perez S, Vereijken JM. Sunflower proteins: overview of their physicochemical, structural and functional properties. J Sci Food Agric. 2007;87:2173-2191.

22. Hudson BJF, ed., New and Developing Sources of Food Proteins, Springer US, Boston, MA, 1994.

23. Wildermuth SR, Young EE, Were LM. Chlorogenic Acid Oxidation and Its Reaction with Sunflower Proteins to Form Green-Colored Complexes: Chlorogenic acid oxidation. Compr Rev Food Sci Food Saf. 2016;15(5):829-843.

24. Bongartz V, Brandt L, Gehrmann ML, Zimmermann BF, Schulze-Kaysers N, Schieber A. Evidence for the Formation of Benzacridine Derivatives in Alkaline-Treated Sunflower Meal and Model Solutions. Molecules. 2016;21(1):91.

25. Weisz GM, Schneider L, Schweiggert U, Kammerer DR, Carle R. Sustainable sunflower processing-I. Development of a process for the adsorptive decolorization of sunflower [Helianthus annuus L.] protein extracts. Innov Food Sci Emerg Technol. 2010;11(4):733-741.

26. Weisz GM, Carle R, Kammerer DR. Sustainable sunflower processing — II. Recovery of phenolic compounds as a by-product of sunflower protein extraction. Innov Food Sci Emerg Technol. 2013;17:169-179.

27. Slabi SA, Mathe C, Framboisier X, Defaix C, Mesieres O, Galet O, et al. A new SE-HPLC method for simultaneous quantification of proteins and main phenolic compounds from sunflower meal aqueous extracts. Anal Bioanal Chem. 2019;411(10):2089-2099.

28. Sara AS, Mathe C, Basselin M, Fournier F, Aymes A, Bianeis M, et al. Optimization of sunflower albumin extraction from oleaginous meal and characterization of their structure and properties. Food Hydrocoll. 2020;99:105335.

29. Yemm EW, Willis A. The estimation of carbohydrates in plant extracts by anthrone. Biochem J. 1954;57(3):508-514.

30. AOCS International., Official method 991.20. Nitrogen (total) in milk. Official methods of analysis, 19th edition, Gaithersburg: AOCS International. 1995.

31. Slabi SA, Mathe C, Basselin M, Framboisier X, Ndiaye M, Galet O, et al. Multi-objective optimization of solid/liquid extraction of total sunflower proteins from cold press meal. Food Chemistry. 2020;317:126423.

32. Farah A, Monteiro M, Donangelo CM, Lafay S. Chlorogenic Acids from Green Coffee Extract are Highly Bioavailable in Humans. The J Nutr. 200;138(12):2309-2315.

33. Ramalakshmi K, Hithamani G, Asha KR, Jagan Mohan Rao L. Separation and characterisation of chlorogenic acid-rich conserves from green coffee beans and their radical scavenging potential: Separation and characterisation of chlorogenic acid.

34. Bishop CT. Carbohydrates of sunflower heads. Can J Chem. 1955;33:1521-1529.

35. Yang Q, Zhao M, Lin L. Adsorption and desorption characteristics of adlay bran free phenolics on macroporous resins. Food Chemistry. 2016;194:900-907.

36. Dong Y, Zhao M, Sun-Waterhouse D, Zhuang M, Chen H, Feng M, et al. Absorption and desorption behaviour of the flavonoids from Glycyrrhiza glabra L. leaf on macroporous adsorption resins. Food Chemistry. 2015;168:538-545.

37. Xu Z, Zhang Q, Chen J, Wang L, Anderson GK. Adsorption of naphthalene derivatives on hypercrosslinked polymeric adsorbents. Chemosphere. 1999;38(9):2003-2011.

38. Sandhu AK, Gu L. Adsorption/Desorption Characteristics and Separation of Anthocyanins from Muscadine (Vitis rotundifolia) Juice Pomace by Use of Macroporous Adsorbent Resins. J Agric Food Chem. 2013;61:1441-1448.

39. Lin L, Zhao H, Dong Y, Yang B, Zhao M. Macroporous resin purification behavior of phenolics and rosmarinic acid from Rabdosia serra (MAXIM.) HARA leaf. Food Chemistry. 2012;130(2):417-424.

40. Lagergren S. About the Theory of So-Called Adsorption of Soluble Substances. Sven Vetenskapsakad Handingarl. 1898;24:1-39.

41. Ho YS, Mckay G. Kinetic Models for the Sorption of Dye from Aqueous Solution by Wood. Process Saf Environ Prot. 1998;76:183-191.

42. Weber WJ, Morris JC. Kinetics of adsorption on carbon from solution. J Sanit Eng Div. 1963;89:31-60.

43. Annadurai G, Krishnan MRV. Adsorption of acid dye from aqueous solution by chitin: Equilibrium studies. Indian J Chem Technol. 1997;4(5):217-222.

44. Firdaous L, Fertin B, Khelissa O, Dhainaut M, Nedjar N, Chataigne G, et al. Adsorptive removal of polyphenols from an alfalfa white proteins concentrate: Adsorbent screening, adsorption kinetics and equilibrium study. Sep Pur Technol. 2017;178:29-39.

45. Tran HN, You SJ, Hosseini-Bandegharaei A, Chao HP. Mistakes and inconsistencies regarding adsorption of contaminants from aqueous solutions: A critical review. Water Research. 2017;120:88-116.

46. Chen Y, Zhang W, Zhao T, Li F, Zhang M, Li J, et al. Adsorption properties of macroporous adsorbent resins for separation of anthocyanins from mulberry. Food Chemistry. 2016;194:712-722.

47. Gok O, Ozcan A, Erdem B, Ozcan AS. Prediction of the kinetics, equilibrium and thermodynamic parameters of adsorption of copper(II) ions onto 8-hydroxy quinoline immobilized bentonite. Colloids Surf A Physicochem Eng Asp. 2008;317:174-185.

48. Gokmen V, Serpen A. Equilibrium and kinetic studies on the adsorption of dark colored compounds from apple juice using adsorbent resin. J Food Eng. 2002;53:221-227.

49. Liu T, Li Y, Du Q, Sun J, Jiao Y, Yang G, et al. Adsorption of methylene blue from aqueous solution by graphene. Colloids Surf B. 2012;90:197-203.

50. Gao ZP, Yu ZF, Yue TL, Quek SY. Adsorption isotherm, thermodynamics and kinetics studies of polyphenols separation from kiwifruit juice using adsorbent resin. J Food

Eng. 2013;116:195-201.

51. Gupta VK. Equilibrium Uptake, Sorption Dynamics, Process Development, and Column Operations for the Removal of Copper and Nickel from Aqueous Solution and Wastewater Using Activated Slag, a Low-Cost Adsorbent. Ind Eng Chem Res. 1998;37:192-202.

52. Ding L, Deng H, Wu C, Han X. Affecting factors, equilibrium, kinetics and thermodynamics of bromide removal from aqueous solutions by MIEX resin. Int J Chem Eng. 2012;181:360-370.

53. Xi L, Mu T, Sun H. Preparative purification of polyphenols from sweet potato (Ipomoea batatas L.) leaves by AB-8 macroporous resins. Food Chemistry. 2015;172:166-174.